Computers, Materials & Continua
DOI:10.32604/cmc.2021.014507
Article

A Computational Analysis to Burgers Huxley Equation

Muhammad Saqib[1], Muhammad Shoaib Arif[2,*], Shahid Hasnain[3] and Daoud S. Mashat[4]

[1]Department of Mathematics, Numl University, Islamabad, 44000, Pakistan
[2]Department of Mathematics, Air University, Islamabad, 44000, Pakistan
[3]Department of Mathematics, Air University, Multan Campus, Multan, 66000, Pakistan
[4]Department of Mathematics, King Abdulaziz University, Jeddah, Saudi Arabia
[*]Corresponding Author: Muhammad Shoaib Arif. Email: shoaib.arif@mail.au.edu.pk
Received: 24 September 2020; Accepted: 04 December 2020

Abstract: The efficiency of solving computationally partial differential equations can be profoundly highlighted by the creation of precise, higher-order compact numerical scheme that results in truly outstanding accuracy at a given cost. The objective of this article is to develop a highly accurate novel algorithm for two dimensional non-linear Burgers Huxley (BH) equations. The proposed compact numerical scheme is found to be free of superiors approximate oscillations across discontinuities, and in a smooth flow region, it efficiently obtained a high-order accuracy. In particular, two classes of higher-order compact finite difference schemes are taken into account and compared based on their computational economy. The stability and accuracy show that the schemes are unconditionally stable and accurate up to a two-order in time and to six-order in space. Moreover, algorithms and data tables illustrate the scheme efficiency and decisiveness for solving such non-linear coupled system. Efficiency is scaled in terms of L_2 and L_∞ norms, which validate the approximated results with the corresponding analytical solution. The investigation of the stability requirements of the implicit method applied in the algorithm was carried out. Reasonable agreement was constructed under indistinguishable computational conditions. The proposed methods can be implemented for real-world problems, originating in engineering and science.

Keywords: Burgers Huxley equation; finite difference schemes; HOC schemes; Thomas algorithm; Von-Neumann stability analysis

1 Introduction

This paper describes the multiplex schemes solution for two dimensional non-linear Burgers Huxley equation. Such an equation serves as the coupling between the Z_{xx}, Z_{yy} diffusive terms and $Z(Z_x + Z_y)$ the convectional phenomena. This equation is of high importance for showing a prototype model describing the interaction between reaction mechanisms, convection effects and diffusion transports. It is the combination of both Burgers & Huxley phenomena with non-linear term means reactions kind of characteristics behaviour, to capture some features of fluid turbulence which caused by the effects of convection & diffusion [1–3]. It is a quantitative paradigm which deals with the flow of electric current through the surface membrane of a giant nerve fibre. Nerve pulse propagation in nerve fibres and wall motion in liquid crystals. Recently research has been measured to investigate two dimensional Burgers Huxley phenomena for understanding the various physical flows in fluid theory [4–6] which leads to implementing a novel methodology for studying new insights [7,8]. It is worth mentioning that there is a vast amount of different approaches available in the literature to calculate the solutions of non-linear systems of partial differential equations. Seeking the Burgers Huxley equations numerical solution, wavelet collocation methods for the solution of Burgers Huxley equations [9] have already been studied in combination with variational iteration technique [10,11]. Moreover, the propagation of genes (Burger & Fisher) and Reaction-Diffusion (Gray Scott) models [12,13] investigated largely by the technique of computation [14]. On the other hand, optimal homotopy asymptotic & homotopy perturbation method was carried out to find the approximate solution of Boussinesq-Burgers equations [15]. Finally, some novel techniques also take into account like chaos theory [16], non-linear optics and fermentation process [17,18]. Wazwaz obtained the solitary wave solutions of one dimensional Burgers Huxley equation using tanh-coth method [19]. Hashim et al. [20,21] using Adomian Decomposition Method. Molabahrami et al. [22] used the homotopy analysis method to find the solution of one dimensional Burger Huxley equation also Efimova et al. [23] find the travelling wave solution of such equation. Batiha et al. [24] used Hope-Cole transformation with Gao et al. [25] find the exact solution of the generalized Burgers equation.

This research aims to deal with higher-order compact schemes with the finite difference methodology [8]. Our primary focus is to attain a compatible scheme which is highly efficient and easy to implement with better accuracy. Although, Burgers Huxley equation can be in three dimensions still some features kept unexplored in the two-dimensional scenario. Let us explorer some new insights in BH equation which consists of the two-dimensional domain which can be written as:

$$\frac{\partial Z}{\partial t} = \Delta Z + \xi Z^{\mu} \nabla Z + \eta Z P_{(\mu,\beta)}(Z), \tag{1}$$

where $Z = Z(l, m, t)$ is the unknown velocity & $(l, m, t) \in \Lambda \times (0\, T]$. Laplacian can be defined as

$$\nabla \equiv \frac{\partial}{l} i + \frac{\partial}{m} j \tag{2}$$

with two dimensional behavior,

$$\Delta \equiv \frac{\partial^2}{l^2} + \frac{\partial^2}{m^2}, \tag{3}$$

also $P_{\mu,\beta} = (Z^{\mu} - 1)(\beta - Z)$ is a non-linear reaction term. The coefficient ξ, η are advection and reactions coefficients accordingly with $0 < \beta < 1$ & $\mu > 0$. These parameters describe the interaction between reaction mechanisms, convection effects & diffusion transports [26,27]. Let us consider the initial condition,

$$Z(x, y, 0) = Z_0(x, y) \quad \text{for} \quad (x, y) \in \Lambda, \tag{4}$$

which can be seen from the upcoming Eq. (12). The Dirichlet boundary conditions are given by,

$$\left.\begin{array}{ll} Z(l,m,t)=p_1(l,m,t), & Z(s,m,t)=p_2(l,m,t) \\ Z(l,c,t)=q_1(l,m,t), & Z(l,d,t)=q_2(l,m,t) \end{array}\right\} (x,y)\in\Lambda. \tag{5}$$

where Λ is a rectangular domain in R^2 & Z_0, p_1, p_2, q_1, q_2 are given sufficiently smooth functions, and $Z(l, m, t)$ may represent unknown velocity, whereas $Z.Z_l$, $Z.Z_m$ represents convection terms along with linear diffusion Z_{ll}, Z_{mm}. Such phenomena perpetuate the ionic mechanisms underlying the initiation and propagation of action potentials in the squid giant axon [28,29].

More generally, it is a challenging task for determining and preservation of physical properties like accuracy, stability, convergence criteria and design efficiency for the given two-dimensional problem. This equation can be an effective procedure for the solution of various deterministic problems in physics, biology and chemical reactions. Also, deals in the investigation of the growth of colonies of bacteria consider population densities or sizes, which are non-negative variables. Most non-linear models of real-life problems are still very challenging to solve either numerically or theoretically. There has recently been much attention devoted to the search for better and more efficient solution methods for determining a solution, analytical or numerical, to non-linear models [30,31]. In [31–34] authors present a method used to solve partial equations with the use of artificial neural networks and an adaptive strategy to collocate them. To get the approximate solution of the partial differential equations Deep Neural Networks (DNNs) has been used, which shows impressive results in areas such as visual recognition [35]. Recently in [36], authors develop a numerical method with third-order temporal accuracy to solve time-dependent parabolic and first-order hyperbolic partial differential equations. We focused on elaborating further by comparing analytical and numerical techniques.

2 Tanh-Coth Method

The dynamical balance between the non-linear reaction term and diffusive effects which constitute stable waveform after colliding with each other. In (1) the negative coefficients of Z_{ll}, Z_{mm} and Z^3 follow the physical behaviour of two dimensional BH Eq. (1). Such an equation can be converted into the non-linear ordinary differential equation which is as follows:

$$eZ' + 2Z'' + 2ZZ' + Z + \gamma Z P_{\mu,\lambda}(Z) = 0 \tag{6}$$

Let $\sigma = x - et$, the wave variable which balances the non-linear reaction term ($\boldsymbol{P}_{\boldsymbol{\mu},\lambda}(\boldsymbol{Z})$) where μ, λ are index values and diffusion transport (the highest derivative involved), we have $M+2=3$, $MM=1$. This enables us to set: Put $M=1$ in (6) we get

$$Z(\sigma) = a_0 + a_1 Y + b_1 Y^{-1} \tag{7}$$

Let $Y = \tanh(\gamma\sigma)$, and $\sigma = ((x+y) - et)$

$$\text{Then,}\quad \left.\begin{array}{l} Z = a_0 + a_1 Y + b_1 Y^{-1} \& Z' = a_1\gamma(1-Y^2) - b_1\gamma(1-Y^2)Y^{-2} \\ Z'' = -2a_1\gamma^2 Y\left(1-Y^2\right) + 2b_1\gamma^2\dfrac{(1-Y^2)^2}{Y^3} + 2\gamma^2 b_1\dfrac{(1-Y^2)}{Y}. \end{array}\right\} \tag{8}$$

Substitutes aforementioned in Eq. (6), we have the following solution to (7)

$$\left.\begin{array}{l}\frac{1}{Y^3}((-a_1^2\gamma+2\gamma^2a_1-a_1^3)Y^6+(-ea_1\gamma-a_0a_1\gamma+\beta a_1^2-3a_0a_1^2+a_1^2)Y^5\\ \quad+(-2a_1\gamma^2+a_1^2\gamma+2a_0a_1\beta-3a_0^2a_1-3a_1^2b_1-a_1\beta+2a_0a_1)Y^4\\ \quad+(ea_1\gamma+eb_1\gamma+a_0a_1\gamma+a_0b_1\gamma+\beta a_0^2+2a_1b_1\beta-a_0^3-6a_0a_1b_1-a_0\beta+a_0^2+2a_1b_1)Y^3\\ \quad+(-4b_1\gamma^2+2\gamma^2b_1+b_1^2\gamma+2a_0b_1\beta-3a_0^2b_1-3a_1b_1^2-b_1\beta+2a_0b_1)Y^2\\ \quad+(-b_1\gamma-a_0b_1\gamma+b_1^2-3a_0b_1^2+\beta b_1^2)Y\\ \quad+(-b_1^3+2\gamma^2b_1-b_1^2\gamma)Y^0)=0\end{array}\right\} \tag{9}$$

Arranging the coefficients of $Y^i, i\geq 0$, and equating these coefficients to zero, the system of algebraic equations in a_0, a_1, b_1, γ and e are obtained. By solving the following set of the algebraic system of equations, we have the following form:

$$\left.\begin{array}{l}Y^0: b_1(b_1+2\gamma)(\gamma-b_1)=0\\ Y^1: b_1((\beta-3a_0+1)-\gamma(a_0+e))=0\\ Y^2: b_1^2(\gamma-3a_1)+b_1(-3a_0^2+(2\beta+2)a_0-2\gamma^2-\beta)=0\\ Y^3: -a_0^3+a_0^2(\beta+1)+((\gamma-6b_1)a_1+b_1\gamma-\beta)a_0+2b_1(\beta+1)a_1+\gamma(ea_1+eb_1)=0\\ Y^4: (-3b_1+\gamma)a_1^2+(-3a_0^2+(2\beta+2)a_0-2\gamma^2-\beta)a_1=0\\ Y^5: (\beta-3a_0+1)a_1^2-a_1\gamma(a_0+e)=0\\ Y^6: a_1(\gamma-a_1)(2\gamma+a_1)=0\end{array}\right\} \tag{10}$$

In Eq. (10), the solution is of the form:

Case 1: We found that $b_1=0$,

$$a_0=\frac{1}{2},\quad a_1=\frac{-1}{2},\quad \gamma=\frac{1}{4},\quad e=\frac{1-4\beta}{2}\quad \&\quad a_0=\frac{\beta}{2},\quad a_1=\frac{-\beta}{2},\quad \gamma=\frac{\beta}{4},\quad e=\frac{\beta-4}{2}$$

$$a_0=\frac{\beta+1}{2},\quad a_1=-\frac{\beta-1}{2},\quad \gamma=\frac{\beta-1}{4},\quad e=\frac{\beta+1}{2}\quad \&\quad a_0=\frac{1}{2},\quad a_1=\frac{1}{2},\quad \gamma=\frac{1}{2},\quad e=\beta-1$$

$$a_0=\frac{\beta}{2},\quad a_1=\frac{\beta}{2},\quad \gamma=\frac{\beta}{2},\quad e=1-\beta\quad \&\quad a_0=\frac{\beta+1}{2},\quad a_1=\frac{\beta-1}{2},\quad \gamma=\frac{\beta-1}{2}, e=-(1+\beta)$$

Case 2: We found that $a_1 = 0$,

$$a_0 = \frac{1}{2},\quad b_1 = \frac{-1}{2},\quad \gamma = \frac{1}{4},\quad e = \frac{1-4\beta}{2} \quad \& \quad a_0 = \frac{\beta}{2},\quad b_1 = \frac{-\beta}{2},\quad \gamma = \frac{\beta}{4},\quad e = \frac{\beta-4}{2}$$

$$a_0 = \frac{\beta+1}{2},\quad b_1 = -\frac{\beta-1}{2},\quad \gamma = \frac{\beta-1}{4},\quad e = \frac{\beta+1}{2} \quad \& \quad a_0 = \frac{1}{2},\quad b_1 = \frac{1}{2},\quad \gamma = \frac{1}{2},\quad e = \beta - 1$$

$$a_0 = \frac{\beta}{2},\quad b_1 = \frac{\beta}{2},\quad \gamma = \frac{\beta}{2},\quad e = 1-\beta \quad \& \quad a_0 = \frac{\beta+1}{2},\quad b_1 = \frac{\beta-1}{2},\quad \gamma = \frac{\beta-1}{2},\quad e = -(1+\beta).$$

From Cases 1 and 2, the kink solution is of the form:

$$Z_1(x,y,t) = \frac{1}{2}\left(1 - tanh\left[\frac{1}{4}\left(x+y-\frac{1-4\beta}{2}t\right)\right]\right) \quad \&$$

$$Z_2(x,y,t) = \frac{\beta}{2}\left(1 - tanh\left[\frac{\beta}{4}\left(x+y-\frac{\beta-4}{2}t\right)\right]\right)$$

$$Z_3(x,y,t) = \frac{\beta+1}{2} - \frac{\beta-1}{2}tanh\left[\frac{\beta-1}{4}\left(x+y-\frac{\beta+1}{2}t\right)\right] \quad \&$$

$$Z_4(x,y,t) = \frac{1}{2}\left(1 + tanh\left[\frac{1}{2}(x+y-(\beta-1)t)\right]\right)$$

$$Z_5(x,y,t) = \frac{\beta}{2}\left(1 + tah\left[\frac{\beta}{2}(x+y-(1-\beta)t)\right]\right) \quad \&$$

$$Z_6(x,y,t) = \frac{\beta+1}{2} + \frac{\beta-1}{2}tanh\left[\frac{\beta-1}{2}(x+y+(1+t)t)\right]$$

$$Z_7(x,y,t) = \frac{1}{2}\left(1 - coth\left[\frac{1}{4}\left(x+y-\frac{1-4\beta}{2}t\right)\right]\right) \quad \&$$

$$Z_8(x,y,t) = \frac{\beta}{2}\left(1 - coth\left[\frac{\beta}{4}\left(x+y-\frac{\beta-4}{2}t\right)\right]\right)$$

$$Z_9(x,y,t) = \frac{\beta+1}{2} - \frac{\beta-1}{2}coth\left[\frac{\beta-1}{4}\left(x+y-\frac{\beta+1}{2}t\right)\right] \quad \&$$

$$Z_{10}(x,y,t) = \frac{1}{2}\left(1 + coth\left[\frac{1}{2}(x+y-(\beta-1)t)\right]\right)$$

$$Z_{11}(x,y,t) = \frac{\beta}{2}\left(1 + coth\left[\frac{\beta}{2}(x+y-(1-\beta)t)\right]\right) \quad \&$$

$$Z_{12}(x,y,t) = \frac{\beta+1}{2} + \frac{\beta-1}{2}coth\left[\frac{\beta-1}{2}(x+y+(1+t)t)\right]$$

Now by solving (1) using the tanh-coth method, the analytical solution (kink solution) is in a compact form in both cases is as follows:

$$Z(\sigma) = a_0 + a_1 tanh(\gamma\sigma) + b_1 tanh(\sigma\gamma)^{-1} \tag{11}$$

with initial condition:

$$Z(x,t,0) = Z_0(x,y) = a_0 + a_1 tanh(\gamma(x+y) + b_1 tanh(\gamma(x+y))^{-1} \tag{12}$$

where Z is the unknown velocity, and γ & σ are wavenumbers which are developed during the solution of BH equation.

3 Description of Compact Schemes

Let us discretize the spatial domain which consists of N and M positive integers, such that h_l and h_m present step sizes along with l and m directions, respectively [37]. The spatial nodes can be denoted by l_i, m_j, namely, $l_i = ih_l$, $i = 0, 1, \ldots, N-1, N$ & $m_j = jh_m$, $j = 0, 1, \ldots, M-1, M$. For the temporal domain, let us take dt as time-step discretization, $\tau = T/dt$, with $t_n = N\tau$. Also $t_{n+1/2} = \dfrac{t_n + t_{n+1}}{2}$ with $N = 0, 1, 2, \ldots, dt-1$ [37–39]. Where τ is the temporal step size. Set $ZZ_\tau = \{w \mid w = (w^0, w^1, w^2, \ldots, w^{dt})^T$, for any $w \in ZZ_\tau$, with some more notations:

$$\left.\begin{aligned} w^{n+1/2} &= \frac{w^{n+1} + w^n}{2} \\ \frac{\partial}{\partial t} w^{n+1/2} &= \frac{w^{n+1} - w^n}{\tau} \end{aligned}\right\} \tag{13}$$

for $n = 0, 1, 2, \ldots, dt-1$.

Implementation Procedure:

Let us we divide (1) into two parts such as:

$$\left.\begin{aligned} -[\delta_l^2 Z_{i,j} + ZZ_l] &= P_{\mu,\beta} - Z_t + \delta_m^2 Z_{i,j} + ZZ_m \\ -[\delta_m^2 Z_{i,j} + ZZ_m] &= P_{\mu,\beta} - Z_t + \delta_l^2 Z_{i,j} + ZZ_l \end{aligned}\right\} (x,y) \in \Lambda, \ \ t > 0 \tag{14}$$

Now considering one-dimensional steady convection-diffusion equation in the following form:

$$\left.\begin{aligned} -\alpha_1 \frac{\partial^2 \omega_{rr}}{\partial l^2} + \beta_1 \frac{\partial \omega_{rr}}{\partial l} &= \overbrace{F} \\ -\alpha_{11} \frac{\partial^2 \omega_{rr}}{\partial m^2} + \beta_{11} \frac{\partial \omega_{rr}}{\partial m} &= \overbrace{F} \end{aligned}\right\} \tag{15}$$

where α_1, α_{11} are the constants while β_1, β_{11} are the convective velocities. $\overbrace{F}$ is the smooth functions of l and m may represent the reaction, vorticity. Now the three-point scheme is as follows:

$$\left.\begin{array}{l} -\left(\alpha_1+\dfrac{\beta_1 h_l^2}{12\alpha_1}\right)\delta_l^2\omega_{rr}(l_i)+\beta_1\Delta_l\omega_{rr}(l_i)=\left[1+\dfrac{h_l^2}{12}\left(\delta_l^2-\dfrac{\beta_1}{\alpha_1}\Delta_l\right)\right]\overbrace{F} \\ -\left(\alpha_{11}+\dfrac{\beta_{11} h_m^2}{12\alpha_{11}}\right)\delta_m^2\omega_{rr}(m_j)+\beta_{11}\Delta_m\omega_{rr}(m_j)=\left[1+\dfrac{h_m^2}{12}\left(\delta_m^2-\dfrac{\beta_{11}}{\alpha_{11}}\Delta_m\right)\right]\overbrace{F} \end{array}\right\} \tag{16}$$

Now applying the Taylor series expansion to Eq. (14) we have the following results:

$$-\left(\alpha_1+\frac{\beta_1^2 h_l^2}{12\alpha_1}\right)\delta_l^2 Z^{n+\frac{1}{2}}+\beta_1\Delta_l Z^{n+\frac{1}{2}}=\left[1+\frac{h_l^2}{12}\left(\delta_l^2-\left(\frac{\beta_1}{\alpha_1}\right)\Delta_m\right)\right]\left[\overbrace{F}-Z_t+\delta_m^2 Z+\beta_1\Delta_l\right]\Bigg\} \tag{17}$$

$$-\left(\alpha_{11}+\frac{\beta_{11}^2 h_m^2}{12\alpha_{11}}\right)\delta_m^2 Z^{n+\frac{1}{2}}+\beta_{11}\Delta_m Z^{n+\frac{1}{2}}=\left[1+\frac{h_m^2}{12}\left(\delta_m^2-\left(\frac{\beta_{11}}{\alpha_{11}}\right)\Delta_m\right)\right]\left[\overbrace{F}-Z_t+\delta_m^2 Z+\beta_{11}\Delta_m\right]\Bigg\} \tag{18}$$

where $0 \le n \le dt-1$ and the truncation error is

$$Residual_{1(i,j)}^{n+1/2}=O(h_l^4+h_m^4), \quad (l,m)\in\Lambda,\ t>0. \tag{19}$$

By adding Eqs. (17) and (18) we have the following form (1) which yields:

$$\left.\begin{array}{l} -\left(\alpha_1+\dfrac{\beta_1^2 h_l^2}{12\alpha_1}\right)\delta_l^2 Z^{n+\frac{1}{2}}+\beta_1\Delta_l Z^{n+\frac{1}{2}}-\left(\alpha_{11}+\dfrac{\beta_{11}^2 h_m^2}{12\alpha_{11}}\right)\delta_m^2 Z^{n+\frac{1}{2}}+\beta_{11}\Delta_m Z^{n+\frac{1}{2}} \\ =\left[1+\dfrac{h_l^2}{12}\left(\delta_l^2-\left(\dfrac{\beta_1}{\alpha_1}\right)\Delta_m\right)\right]\left[\overbrace{F}-Z_t+\delta_m^2 Z+\beta_1\Delta_y\right]+\left[1+\dfrac{h_m^2}{12}\left(\delta_m^2-\left(\dfrac{\beta_{11}}{\alpha_{11}}\right)\Delta_m\right)\right] \\ \left[\overbrace{F}-Z_t+\delta_m^2 Z+\beta_{11}\Delta_m\right]+Residual_{1(i,j)}^{n+1/2} \end{array}\right\} \tag{20}$$

where $Residual_{1(i,j)}^{n+1/2}=O(h_l^4+h_m^4)$, $(l,m)\in\Lambda,\ t>0$.

Apply Crank–Nicholson time discretization, which leads to:

$$\left.\begin{aligned}
&\frac{1}{2}\left[\alpha_1+\frac{\beta_1^2h_l^2}{12\alpha_1}\right]\delta_l^2Z_{i,j}^{n+1}+\frac{1}{2}\left[\alpha_{11}+\frac{\beta_{11}^2h_m^2}{12\alpha_{11}}\right]\delta_m^2Z_{i,j}^{n+1}-\frac{1}{2}\beta_1\Delta_lZ_{i,j}^{n+1}+\frac{1}{2}\beta_{11}\Delta_mZ_{i,j}^{n+1}\\
&+\frac{1}{\tau}\left[1+\frac{h_l^2}{12}\left(\delta_l^2-\left(\frac{\beta_1}{\alpha_1}\right)\Delta_l\right)\right]Z_{i,j}^{n+1}+\frac{1}{\tau}\left[1+\frac{h_m^2}{12}\left(\delta_m^2-\left(\frac{\beta_{11}}{\alpha_{11}}\right)\Delta_m\right)\right]Z_{i,j}^{n+1}\\
&+\frac{1}{2}\left[1+\frac{h_l^2}{12}\left(\delta_l^2-\left(\frac{\beta_1}{\alpha_1}\right)\Delta_l\right)\right]\delta_m^2Z_{i,j}^{n+1}+\frac{1}{2}\left[1+\frac{h_m^2}{12}\left(\delta_m^2-\left(\frac{\beta_{11}}{\alpha_{11}}\right)\Delta_m\right)\right]\delta_l^2Z_{i,j}^{n+1}\\
&+\frac{1}{2}\left[1+\frac{h_l^2}{12}\left(\delta_l^2-\left(\frac{\beta_1}{\alpha_1}\right)\Delta_l\right)\right]\beta_1\Delta_mZ_{i,j}^{n+1}-\frac{1}{2}\left[1+\frac{h_m^2}{12}\left(\delta_m^2-\left(\frac{\beta_{11}}{\alpha_{11}}\right)\Delta_m\right)\right]\beta_{11}\Delta_lZ_{i,j}^{n+1}\\
&=\left[1+\frac{h_l^2}{12}\left(\delta_l^2-\frac{\beta_1}{\alpha_1}\Delta_l\right)\right]F^{n+\frac{1}{2}}+\left[1+\frac{h_m^2}{12}\left(\delta_m^2-\frac{\beta_{11}}{\alpha_{11}}\Delta_m\right)\right]F^{n+\frac{1}{2}}\\
&\quad+\frac{1}{\tau}\left[1+\frac{h_l^2}{12}\left(\delta_l^2-\left(\frac{\beta_1}{\alpha_1}\right)\Delta_l\right)\right]Z_{i,j}^{n}\\
&\quad+\frac{1}{\tau}\left[1+\frac{h_m^2}{12}\left(\delta_m^2-\left(\frac{\beta_{11}}{\alpha_{11}}\right)\Delta_m\right)\right]Z_{i,j}^{n}+\frac{1}{2}\left[1+\frac{h_l^2}{12}\left(\delta_l^2-\left(\frac{\beta_1}{\alpha_1}\right)\Delta_l\right)\right]\delta_m^2Z_{i,j}^{n}\\
&\quad+\frac{1}{2}\left[1+\frac{h_m^2}{12}\left(\delta_m^2-\left(\frac{\beta_{11}}{\alpha_{11}}\right)\Delta_m\right)\right]\delta_l^2Z_{i,j}^{n}\\
&\quad+\frac{1}{2}\left[1+\frac{h_l^2}{12}\left(\delta_l^2-\left(\frac{\beta_1}{\alpha_1}\right)\Delta_l\right)\right]\beta_1\Delta_mZ_{i,j}^{n}+\frac{1}{2}\left[1+\frac{h_m^2}{12}\left(\delta_m^2-\left(\frac{\beta_{11}}{\alpha_{11}}\right)\Delta_m\right)\right]\beta_{11}\Delta_lZ_{i,j}^{n}\\
&\quad+\frac{1}{2}\left[\alpha_1+\frac{\beta_1^2h_l^2}{12\alpha_1}\right]\delta_l^2Z_{i,j}^{n}-\frac{1}{2}\left[\alpha_{11}+\frac{\beta_{11}^2h_m^2}{12\alpha_{11}}\right]\delta_m^2Z_{i,j}^{n}+\frac{1}{2}\beta_1\Delta_lZ_{i,j}^{n}-\frac{1}{2}\beta_{11}\Delta_mZ_{i,j}^{n}+Residual_{(i,j)}^{n}
\end{aligned}\right\}\quad(21)$$

where $Residual_{(i,j)}^{n}=O(h_l^4+h_m^4+\tau^2)$ represents the truncation error [36–39]. The existence and uniqueness of the solutions of the scheme (21) can be easily found by positive definite property. By applying operators and simplifying the (21) in compact form, The scheme is a system of linear equations based on variable $Z_{i,j}^{n}$, then after applying operators 21 can be written in the following way:

$$\left.\begin{aligned}
&T_1Z_{i,j}^{n+1}+T_2Z_{i+1,j}^{n+1}+T_3Z_{i-1,j}^{n+1}+T_4Z_{i,j+1}^{n+1}+T_5Z_{i,j-1}^{n+1}+T_6Z_{i+1,j+1}^{n+1}+T_7Z_{i-1,j+1}^{n+1}\\
&\quad+T_8Z_{i+1,j-1}^{n+1}+T_9Z_{i-1,j-1}^{n+1}=T_{11}Z_{i,j}^{n}+T_{22}Z_{i+1,j}^{n}+T_{33}Z_{i-1,j}^{n}+T_{44}Z_{i,j+1}^{n}+T_{55}Z_{i,j-1}^{n}\\
&\quad+T_{66}Z_{i+1,j+1}^{n}+T_{77}Z_{i-1,j+1}^{n}+T_{88}Z_{i+1,j-1}^{n}+T_{99}Z_{i-1,j-1}^{n}+ff_1F_{i,j}^{n+\frac{1}{2}}+ff_2F_{i+1,j}^{n+\frac{1}{2}}+ff_3F_{i-1,j}^{n+\frac{1}{2}}\\
&\quad+ff_4F_{i,j+1}^{n+\frac{1}{2}}+ff_5F_{i,j-1}^{n+\frac{1}{2}}
\end{aligned}\right\}\quad(22)$$

where T_1, T_{11}, T_2, T_{22}, ff_1, ..., are all constants coefficients of $Z_{i,j}^{n+1}$, $Z_{i,j}^{n}$ and $ff_{i,j}^{n+\frac{1}{2}}$ which includes α_1, α_{11}, β_1, β_{11}, h_l, h_m, τ and constant values. Let $Z_j = [Z_{1,j} Z_{2,j} \dots Z_{M-1,j}]^{transpose}$ where $0 \le j \le M$. The matrix form of the compact scheme is as follows

$$D_1 Z_j^{n+1} + D_2 Z_{j+1}^{n+1} + D_3 Z_{j-1}^{n+1} = D_{11} Z_j^n + D_{22} Z_{j+1}^n + D_{33} Z_{j-1}^n + f1 F_j^{n+\frac{1}{2}} + f_2 F_{j+1}^{n+\frac{1}{2}} + f_3 F_{j-1}^{n+\frac{1}{2}} \Big\} \tag{23}$$

By calculating and simplifying the terms, we have the following tridiagonal matrix if of the form:

$$\begin{pmatrix} D_1 & D_2 & & & \\ D_3 & D_1 & D_2 & & \\ & \ddots & \ddots & \ddots & \\ & & D_3 & D_1 & D_2 \\ & & & D_3 & D_1 \end{pmatrix} \begin{pmatrix} Z_1^{n+1} \\ Z_2^{n+1} \\ \vdots \\ Z_{M-2}^{n+1} \\ Z_{M-1}^{n+1} \end{pmatrix} = \begin{pmatrix} D_{11} & D_{22} & & & \\ D_{33} & D_{11} & D_{22} & & \\ & \ddots & \ddots & \ddots & \\ & & D_{33} & D_{11} & D_{22} \\ & & & D_{33} & D_{11} \end{pmatrix} \begin{pmatrix} Z_1^{n} \\ Z_2^{n} \\ \vdots \\ Z_{M-2}^{n} \\ Z_{M-1}^{n} \end{pmatrix}$$

$$+ \begin{pmatrix} f_1 & f_2 & & & \\ f_3 & f_1 & f_2 & & \\ & \ddots & \ddots & \ddots & \\ & & f_3 & f_1 & f_2 \\ & & & f_3 & f_1 \end{pmatrix} \begin{pmatrix} f_1^{n+\frac{1}{2}} - D_2 Z_0 \\ f_2^{n+\frac{1}{2}} \\ \vdots \\ f_{M-2}^{n+\frac{1}{2}} \\ f_{M-1}^{n+\frac{1}{2}} - D_2 Z_M \end{pmatrix}$$

where D_{11} matrix is the same as the matrix D_{33}. The Eq. (23) is a tridiagonal block matrix.

$$XZ_{i,j}^{n+1} = QZ_{i,j}^n + Rf_{i,j}^{n+1} \tag{24}$$

The matrix we have generated is diagonally dominant and can solve through Thomas algorithm. Which authenticate the consistency & accuracy of the solution of the form $O(h_l^4 + h_m^2 + \tau^2)$.

4 Description of Six order Compact Finite Difference Scheme

For complex systems the results will be dependent on the formation of the mesh, We apply higher-order compact scheme at the system in Eq. (1) with a uniform mesh at $\Delta l = \Delta m = h_l = h_m$. Scheme description is as follows:

Interior Boundary Points:

The compact schemes at interior boundary points are as follows:

$$\left.\begin{aligned}
&\Lambda_{o(ll)} = \lambda_o \Lambda''_{o(i-1,:)} + \Lambda''_{o(i,:)} + \lambda_o \Lambda''_{o(i+1,:)} = \frac{a_0}{4h_l^2}\left(\Lambda_{o(i+2,:)} - 2\Lambda_{o(i,:)} + \Lambda_{0(i-2,:)}\right) \\
&\quad + \frac{a_1}{h_l^2}\left(\Lambda_{o(i+1,:)} - 2\Lambda_{o(i,:)} + \Lambda_{o(i-1,:)}\right) \\
&\Lambda_{o(mm)} = \lambda_o \Lambda''_{o(:,j-1)} + \Lambda''_{o(:,j)} + \lambda_o \Lambda''_{o(:,j+1)} = \frac{a_0}{4h_m^2}\left(\Lambda_{o(:,j+2)} - 2\Lambda_{o(:,j)} + \Lambda_{o(:,j-2)}\right) \\
&\quad + \frac{a_1}{h_m^2}\left(\Lambda_{o(:,j+1)} - 2\Lambda_{o(:,j)} + \Lambda_{o(:,j-1)}\right) \\
&\Lambda_{o(l)} = \lambda_o \Lambda'_{o(i-1,:)} + \Lambda'_{o(i,:)} + \lambda_o \Lambda'_{o(i+1,:)} = \frac{a_0}{4h_l}(\Lambda_{o(i+2,:)} - \Lambda_{0(i-2,:)}) \\
&\quad + \frac{a_1}{2h_l}(\Lambda_{o(i+1,:)} - \Lambda_{o(i-1,:)}) - \Lambda_{o(i-1,:)}) \\
&\Lambda_{o(m)} = \lambda_o \Lambda'_{o(:,j-1)} + \Lambda'_{o(:,j)} + \lambda_o \Lambda'_{o(:,j+1)} = \frac{a_0}{4h_m}(\Lambda_{o(:,j+2)} - \Lambda_{o(:,j-2)}) \\
&\quad + \frac{a_1}{2h_m}(\Lambda_{o(:,j+1)} - \Lambda_{o(:,j-1)})
\end{aligned}\right\} \tag{25}$$

Above schemes in Eq. (25) constitute λ_o family of tridiagonal structure with parametric values $a_1 = \frac{4}{3}(1 - \lambda_o)$ & $a_0 = \frac{1}{3}(-1 + 10\lambda_o)$. For $\lambda_o = 0$, we get fourth-order accurate scheme while using $\lambda_o = 2/11$, the scheme becomes sixth-order accurate which leads to $a_1 = \frac{12}{11}$ & $a_0 = \frac{3}{11}$ [36–39]. Also, near boundary points, we have to construct a sixth-order compact scheme to sustain accuracy throughout the two-dimensional domain [36–39].

First Boundary Point 1:

At the first boundary point, the six order compact scheme is of the following form.

$$\left.\begin{aligned}
&\Lambda''_{o(1,:)} + \lambda_o \Lambda''_{o(2,:)} = \frac{1}{h^2}(d_1\Lambda_{o(1,:)} + d_2\Lambda_{o(2,:)} + d_3\Lambda_{o(3,:)} + d_4\Lambda_{o(4,:)} + d_5\Lambda_{o(5,:)} + d_6\Lambda_{o(6,:)} + d_7\Lambda_{o(7,:)}) \\
&\Lambda''_{o(:,1)} + \lambda_o \Lambda''_{o(:,2)} = \frac{1}{h^2}(d_1\Lambda_{o(:,1)} + d_2\Lambda_{o(:,2)} + d_3\Lambda_{o(:,3)} + d_4\Lambda_{o(:,4)} + d_5\Lambda_{o(:,5)} + d_6\Lambda_{o(:,6)} + d_7\Lambda_{o(:,7)}) \\
&\Lambda'_{o(1,:)} + \lambda_o \Lambda'_{o(2,:)} = \frac{1}{h}(d_1\Lambda_{o(1,:)} + d_2\Lambda_{o(2,:)} + d_3\Lambda_{o(3,:)} + d_4\Lambda_{o(4,:)} + d_5\Lambda_{o(5,:)} + d_6\Lambda_{o(6,:)} + d_7\Lambda_{o(7,:)}) \\
&\Lambda'_{o(:,1)} + \lambda_o \Lambda'_{o(:,2)} = \frac{1}{h}(d_1\Lambda_{o(:,1)} + d_2\Lambda_{o(:,2)} + d_3\Lambda_{o(:,3)} + d_4\Lambda_{o(:,4)} + d_5\Lambda_{o(:,5)} + d_6\Lambda_{o(:,6)} + d_7\Lambda_{o(:,7)})
\end{aligned}\right\} \tag{26}$$

Above system in Eq. (26), the coefficients can be found by matching Taylor's series expansion comparing with various orders up to order O^7, as a result, construction of the linear system is obtained. By constructing the linear system values of $d's$, which can be solved in the usual way to get the following along l direction, $d_1 = \frac{2077}{157}$, $d_2 = \frac{-2943}{110}$, $d_3 = \frac{573}{44}$, $d_4 = \frac{167}{99}$, $c_5 = \frac{-18}{11}$, $d_6 = \frac{57}{110}$, $d_7 = \frac{-131}{280}$, $\lambda_o = \frac{126}{11}$ [36,37]. Others ones can found in the same way.

2nd Boundary Point 2:

$$\left.\begin{aligned}
&\lambda_o \Lambda''_{o(1,:)} + \Lambda''_{o(2,:)} + \lambda_o \Lambda''_{o(3,:)} = \frac{1}{h^2}\left(d_1 \Lambda_{o(1,:)} + d_2 \Lambda_{o(2,:)} + d_3 \Lambda_{o(3,:)} + d_4 \Lambda_{o(4,:)} + d_5 \Lambda_{o(5,:)}\right.\\
&\quad \left. + d_6 \Lambda_{o(6,:)} + d_7 \Lambda_{o(7,:)}\right)\\
&\lambda_o \Lambda''_{o(:,1)} + \Lambda''_{o(:,2)} + \lambda_o \Lambda''_{o(:,3)} = \frac{1}{h^2}\left(d_1 \Lambda_{o(:,1)} + d_2 \Lambda_{o(:,2)} + d_3 \Lambda_{o(:,3)} + d_4 \Lambda_{o(:,4)} + d_5 \Lambda_{o(:,5)}\right.\\
&\quad \left. + d_6 \Lambda_{o(:,6)} + d_7 \Lambda_{o(:,7)}\right)\\
&\lambda_o \Lambda'_{o(1,:)} + \Lambda'_{o(2,:)} + \lambda_o \Lambda'_{o(3,:)} = \frac{1}{h}\left(d_1 \Lambda_{o(1,:)} + d_2 \Lambda_{o(2,:)} + d_3 \Lambda_{o(3,:)} + d_4 \Lambda_{o(4,:)} + d_5 \Lambda_{o(5,:)}\right.\\
&\quad \left. + d_6 \Lambda_{o(6,:)} + d_7 \Lambda_{o(7,:)}\right)\\
&\lambda_o \Lambda'_{o(:,1)} + \Lambda'_{o(:,2)} + \lambda_o \Lambda'_{o(:,3)} = \frac{1}{h}\left(d_1 \Lambda_{o(:,1)} + d_2 \Lambda_{o(:,2)} + d_3 \Lambda_{o(:,3)} + d_4 \Lambda_{o(:,4)} + d_5 \Lambda_{o(:,5)}\right.\\
&\quad \left. + d_6 \Lambda_{o(:,6)} + d_7 \Lambda_{o(:,7)}\right)
\end{aligned}\right\} \quad (27)$$

Above system in Eq. (27), by constructing the linear system values of $d's$, which can be solved in the usual way to get the following along l direction, $d_1 = \frac{585}{512}$, $d_2 = \frac{-141}{64}$, $d_3 = \frac{459}{512}$, $d_4 = \frac{9}{32}$, $c_5 = \frac{-81}{512}$, $d_6 = \frac{3}{64}$, $d_7 = \frac{-3}{512}$, $\lambda_o = \frac{11}{128}$ [36–39]. Others ones can found in the same way.

Nth Boundary Point:

At Nth boundary point of six order compact scheme is of the following way:

$$\left.\begin{aligned}
&\lambda_o\Lambda''_{o(N-1,:)}+\Lambda''_{o(N,:)}=\frac{1}{h^2}\big(d_1\Lambda_{o(N,:)}+d_2\Lambda_{o(N-1,:)}+d_3\Lambda_{o(N-2,:)}+d_4\Lambda_{o(N-3,:)}\\
&\quad+d_5\Lambda_{o(N-4,:)}+d_6\Lambda_{o(N-5,:)}+d_7\Lambda_{o(N-6,:)}\big)\\
&\lambda_o\Lambda''_{o(:,N-1)}+\Lambda''_{o(:,N)}=\frac{1}{h^2}\big(d_1\Lambda_{o(:,N)}+d_2\Lambda_{o(:,N-1)}+d_3\Lambda_{o(:,N-2)}+d_4\Lambda_{o(:,N-3)}\\
&\quad+d_5\Lambda_{o(:,N-4)}+d_6\Lambda_{o(:,N-5)}+d_7\Lambda_{o(:,N-6)}\big)\\
&\lambda_o\Lambda'_{o(N-1,:)}+\Lambda'_{o(N,:)}=\frac{1}{h}\big(d_1\Lambda_{o(N,:)}+d_2\Lambda_{o(N-1,:)}+d_3\Lambda_{o(N-2,:)}+d_4\Lambda_{o(N-3,:)}\\
&\quad+d_5\Lambda_{o(N-4,:)}+d_6\Lambda_{o(N-5,:)}+d_7\Lambda_{o(N-6,:)}\big)\\
&\lambda_o\Lambda'_{o(:,N-1)}+\Lambda'_{o(:,N)}=\frac{1}{h}\big(d_1\Lambda_{o(:,N)}+d_2\Lambda_{o(:,N-1)}+d_3\Lambda_{o(:,N-2)}+d_4\Lambda_{o(:,N-3)}\\
&\quad+d_5\Lambda_{o(:,N-4)}+d_6\Lambda_{o(:,N-5)}+d_7\Lambda_{o(:,N-6)}\big)
\end{aligned}\right\}\tag{28}$$

Above system in Eq. (28), by constructing the linear system values of $d's$, which can be solved in the usual way as done in boundary point 1 and 2.

Implementation Algorithm:

By arranging Eqs. (26)–(28) in the following algorithm:

$$\left.\begin{aligned}
&\Lambda_{o(ll),j}=\frac{1}{(\Delta l)^2}C^{-1}D\Lambda_{o(j)},\ \ (I_x-\frac{1}{2}\frac{\Delta t}{(\Delta l)^2}C^{-1}D)\Lambda^{\star}_{o(j)}\\
&=\Lambda^n_{o(j)}+\frac{1}{2}\Delta t[\Lambda^n_{o(mm)(,j)}+P(\Lambda^n_{o(i,j)},\Lambda^n_{r(i,j)})](I_l-\frac{1}{2}\frac{\Delta t}{(\Delta l)^2}A^{-1}B)\Lambda^{n+1}_{o(i,)}\\
&=\Lambda^{\star}_{o(i,)}+\frac{1}{2}\Delta t[\Lambda^{\star}_{o(ll)(i,)}+P(\omega^n_{o(i,j)},\Lambda^n_{r(i,j)})],
\end{aligned}\right\}\tag{29}$$

where P are mentioned in Eq. (1), also matrices A and B are $N_m\times N_m$ sparse with triangular nature along C and D are $N_l\times N_l$ sparse with triangular in shape.

Theorem:

The truncation error in the compact six order finite difference scheme for equations in the system (1) is,

$$R^n_{(i,j)}=O\left(h_x^6+h_y^6+\tau^2\right),\quad (l,m)\in\Lambda,\ \ t\geq 0\ [36–40].\tag{30}$$

4.1 Error Analysis

The convergence benchmark, efficiency and accuracy of the proposed scheme in terms of norms can be defined as:

$$L_{\infty Z} = \max_{1 \le o \le L} \max_{1 \le q \le M} \sum_{o=1}^{L} \sum_{q=1}^{M} |(Z_{o,q}^{exact} - Z_{o,q}^{approx})| \tag{31}$$

$$Relative\,Error = \sqrt{\frac{\sum_{i,j=1}^{L} (Z_{i,j}^{exact} - Z_{i,j}^{approx})^2}{\sum_{i,j=1}^{L} (Z_{i,j}^{exact})^2}} \tag{32}$$

$$L_2(w.r.t.Z) = \sqrt{\rho (u_{o,q,k}^{exact} - u_{o,q,k}^{approx})^t (Z_{o,q}^{exact} - Z_{o,q}^{approx})} \tag{33}$$

where $Z_{o,q}^{exact}$ denoted as an analytical solution while $Z_{o,q}^{approx.}$ represents the numerical solution by mesh points (l_o, m_q, t_n). In this experiment $\rho(u_{o,q,k}^{exact} - u_{o,q,k}^{approx}) = \max(\lambda\lambda)$, where $\lambda\lambda$ is an eigenvalue of $(u_{o,q,k}^{exact} - u_{o,q,k}^{approx})$ respectively.

4.2 Stability Analysis

The stability is concerned with the growth or decay of the error produced in the finite-difference solution. For the representation of theoretical analysis, we set $P = 0$ in Eq. (1). Assuming the boundary conditions are accurately propagating, we can apply the Fourier analysis method to our proposed equation.

Definition: For a time-dependent PDE, the corresponding difference scheme is stable in the norm $\|.\|$ if there exists a constant M such that

$$\|e^n\| \le M\|e^0\|, \quad for\ all\ n\nabla t \le t_F$$

where M is independent of ∇t, ∇x and initial condition e^0.

Following the Von Neumann stability analysis criteria, fix the non-linear terms so that for linear stability, the numerical solution can be displayed in the following way:

$$Q_{i,j}^n = \Gamma^n e^{\sqrt{-1}(i\Phi_l h_l + j\Phi_m h_m)} \tag{34}$$

where Γ is the amplitude at time level n, $\sqrt{-1}$ is called the imaginary unit. Φ_l, Φ_m leads to wave number in l, and m directions with $\Phi_l h_l$, $\Phi_m h_m$ are phase angles. The amplification factor is defined by

$$E(\Phi_l, \Phi_m, \tau) = \frac{\zeta^{n+1}}{\zeta^n} \tag{35}$$

By using Eqs. (30) and (35) and dividing by r.h.s of Eq. (35) and simplifying, we have the following form:

$$\left.\begin{array}{l}\Gamma^{n+1}\{T_1+T_2e^{I(l\Phi_l h_l)}+T_3e^{I(-l\Phi_l h_l)}+T_4e^{I(j\Phi_m h_m)}T_5e^{I(-j\Phi_m h_m)}+T_6e^{I(l\Phi_l h_l+m\Phi_m h_m)}+\\ T_7e^{I(-l\Phi_l h_l+m\Phi_m h_m)}T_8e^{I(l\Phi_l h_l-m\Phi_m h_m)}+T_9e^{I(-l\Phi_l h_l-m\Phi_m h_m)}\}\\ =\Gamma^n\{T_{11}+T_{22}e^{I(l\Phi_l h_l)}+T_{33}e^{I(-l\Phi_l h_l)}+T_{44}e^{I(j\Phi_m h_m)}+T_{55}e^{I(-j\Phi_m h_m)}+T_{66}e^{I(l\Phi_l h_l+m\Phi_m h_m)}\\ \quad+T_{77}e^{I(-l\Phi_l h_l+m\Phi_m h_m)}T_{88}e^{I(l\Phi_l h_l-m\Phi_m h_m)}+T_{99}e^{I(-l\Phi_l h_l-m\Phi_m h_m)}\}\end{array}\right\} \tag{36}$$

where $I=\sqrt{-1}$ and Eq. (37) is of the following way:

$$\frac{\Gamma^{n+1}}{\Gamma^n}=\frac{R}{S} \tag{37}$$

where R & S are the compact forms of Eq. (37). For stability, it has to satisfy the following condition:

$$|E(\Phi_l,\Phi_m,\tau)|\le 1 \tag{38}$$

After simplification to an aforementioned condition which holds true. Therefore, $|E|\le 1$ [38–41]. Hence the scheme is unconditionally stable.

5 Experimental Results

The novel numerical scheme is compared with the analytical results of Eq. (1) by using tanh-coth method. For this objective, we consider the same parameter $\alpha=\mu=\eta=1$, and varying β. Numerical and analytic solutions are compared and justified in term of error norms to magnify the importance of higher accuracy.

Furthermore, to avoid turbulence, by varying β values in the Tab. 1 with grid size (15×15), $dt=0.001$ and grid space =0.3125 with respect to $time=1$ is observed. Improvement in accuracy is noted by varying the values of β parameter. Also, the BH equation produced the best results by using six order compact finite difference scheme. At different β values, Tab. 2 indicates error which increased at a very low rate by changing the values of β from high to low which make the comparison to previous work give authentication for accuracy [34]. The truncation error is calculated in Tab. 3, using L_2, $Relative_{error}$ and L_∞ with fixed grid size (31×31). By changing time steps $dt=0.001$ with the same grid size showed results in the Tab. 4. The approximate results using six order compact scheme correspond to error norm are shown in the Tab. 6. In this, table the comparison of fourth-order and six order are analyzed by refining the temporal space, which shows this scheme is better than the corresponding fourth-order. In the Tab. 7 six order and fourth-order compact finite difference scheme comparison is carried out which measured in term of L_∞ norm. Different parameters are also observed under the same scheme. In the Tab. 8 scheme efficiency encountered using L_∞, L_2 & $Relative_{error}$ norms. Graphical representation of numerical schemes on BH equation is observed. Comparison of analytical and numerical results by using fourth and sixth-order compact finite difference scheme has been analyzed. At $t=2$, $\beta=0.1$, $dt=0.0001$, $grid=(21\times 21)$ can be seen from the Fig. 1. While six order scheme at $\beta=0.1$ with time-space $dt=0.0001$ and grid space (21×21) is seen from the Fig. 2 which shows more accurate and refine results as compared with Fig. 1 using the same parameter. In Figs. 3 and 4, analysis shows that the error norm using fourth-order scheme at $\beta=0.001$. While in Fig. 5, we choose

$\beta = 0.0001$ using a higher-order scheme to analyze error profile at grid size (51×51). In summary, it is aspirant from the figures and tables; the analytical and numerical solutions are best fitted with generation encrypting. In the end, the novel six order compact scheme is the best agreement with the analytical solution.

Comparison between approximation and analytical solutions is made at the final time of computation $time = 2\ s$ at the critical point (1, 1) using fourth-order compact scheme at grid size (15×15).

Table 1: Fourth-order compact scheme

Numerical solution at $\alpha = \eta = \mu = 1$, $dt = 0.001$, $h = 0.3125$			
β	Z_{exact}	$Zapprox$	$\lvert Z_{exact} - Z_{approx}\rvert$
0.5	4.0448	4.4171	4.9715e−04
0.1	0.5467	0.5463	4.210e−04
.01	0.8794	0.8792	3.717e−04
.001	0.8972	0.8970	2.29e−04
.0001	0.8989	0.8987	2.27e−04

Comparison between approximation and analytical solutions is made at the final time of computation $time = 1$ at the critical point (1, 1) using fourth-order compact scheme at grid size (31×31).

Table 2: Six order compact scheme

Numerical solution at $\alpha = \eta = \mu = 1$, $dt = 0.0001$, $h = 0.3125$				Present work	CSC method (34)
β	Z_{exact}	$Zapprox$	$\lvert Z_{exact} - Z_{approx}\rvert$	$L_\infty - Z$	L_∞
0.5	0.006792	0.006693	1.66203e−07	6.1461e−08	$6.073 \times 10{-}5$
0.2	0.497500	0.497493	6.2248e−06	5.9791e−07	$3.421 \times 10{-}5$
0.1	0.268941	0.268938	2.94916e−06	5.3642e−07	$1.076 \times 10{-}4$
.01	0.475020	0.475014	5.985021e−06	6.2480e−06	

Table 3: $O(dt^2 + h_l^4 + h_m^4)$

Error estimation at a different time at $dt = 0.001$, $\beta = 0.001$					
Time t	L_2	R_{error}	L_∞	Self-time (s)	Total time (s)
0.1	2.124	3.8013	3.79993	8.428	23.34
0.05	2.123	3.7999	3.79989	20.345	48.456
0.025	2.018	3.7508	3.74980	35.234	70.431
0.0125	1.918	3.74981	3.74970	50.761	101.342
0.005	1.723	3.3.74898	3.74890	100.345	202.451

Table 4: $O(dt^2 + h_l^6 + h_m^6)$

Error estimation at a different time at $dt = 0.001$, $\beta = 0.0001$					
Time t	L_2	R_{error}	L_∞	Self-time (s)	Total time (s)
.1	5.4109	6.2484e−06	6.2474e−06	7.214	22.341
.05	5.2312	6.2482e06	6.2472e−05	4.213	13.561
.025	5.1345	6.2480e05	6.2470e−05	2.341	7.112
.0125	5.0234	6.2470e05	6.2459e−05	1.10	3.561
.005	4.9081	6.2419e−05	5.2494e−05	0.55	1.123

Tab. 3 shows error profile data by using fourth-order compact scheme at $gridsize = (31 \times 31)$ for unknown value $Z(l, m, t)$. *Selftime*: is the time spent in a function excluding the time spent in its child functions while *Totaltime* is the time to execute the algorithm.

Tab. 4 shows error profile data by using Six order compact scheme at $gridsize = (31 \times 31)$ for unknown value $Z(l, m, t)$.

Tab. 5 shows a comparison of two schemes at $gridsize = (51 \times 51)$ and $\beta = 0.001$ for unknowns $Z(l, m, t)$.

Tab. 6 shows a comparison of two schemes at $gridsize = (41 \times 41)$ for unknowns $Z(l, m, t)$.

Table 5: Error comparison

Comparison of two schemes at $dt = 0.1$ at different times level		
	FourthOrder	*SixOrder*
Time-space	$L_\infty - Z$	$L_\infty - Z$
5	6.2241e−04	6.2249e−06
2	5.2449e−04	6.2240e−06
1	4.98e−03	6.2279e−05
0.5	4.97e−03	6.2239e−04

Table 6: Error comparison

Comparison of two schemes at $t = 5$ s, $dt = 0.01$ at different β level		
	FourthOrder	*SixOrder*
β	$L_\infty - Z$	$L_\infty - Z$
.1	3.7494e−04	3.7500e−06
.01	5.9993e−04	5.9998e−06
.001	6.2250e−04	6.2250e−06
.0001	6.2474e−04	6.2475e−06

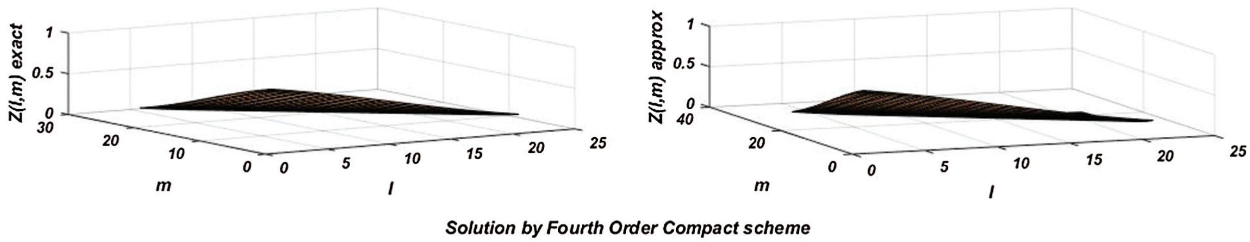

Figure 1: Results obtained by using 4th order scheme at $dt = 0.00011$ & $\beta = 0.1$ at time $= 5$

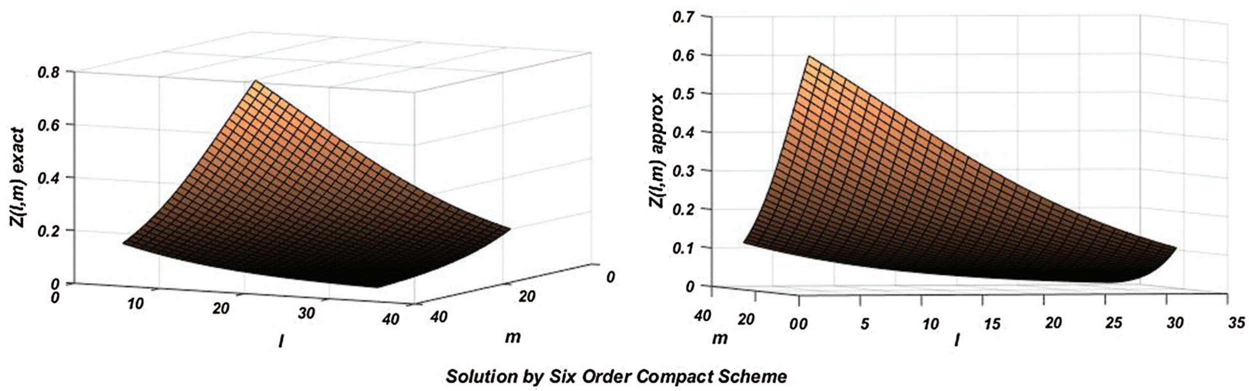

Figure 2: Results which obtained by using 6th order scheme at $dt = 0.0001$, & $\beta = 0.1$ at a time level 2

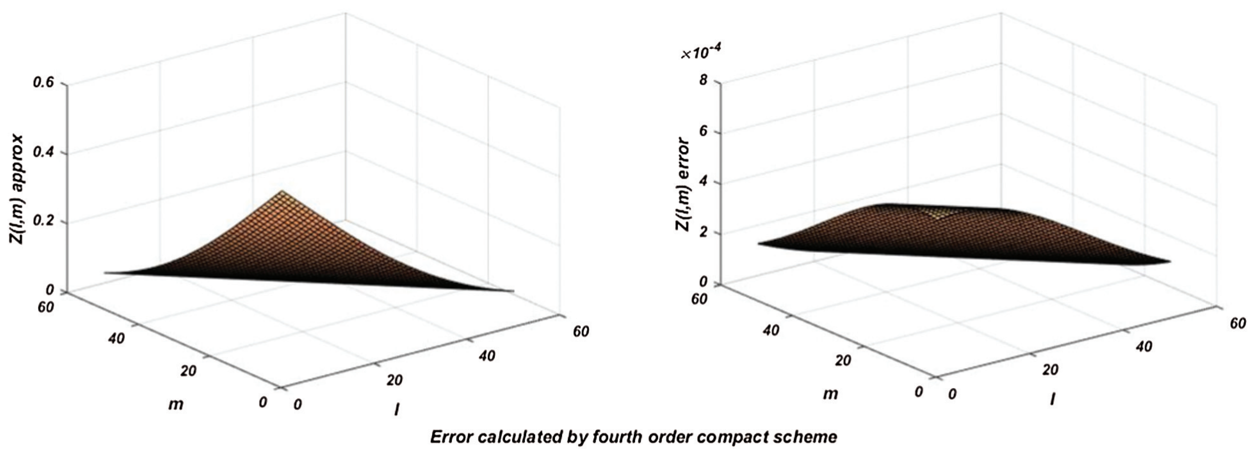

Figure 3: Results for error estimation by using 4th order scheme at $dt = 0.001$ & $\beta = 0.001$ at time 1

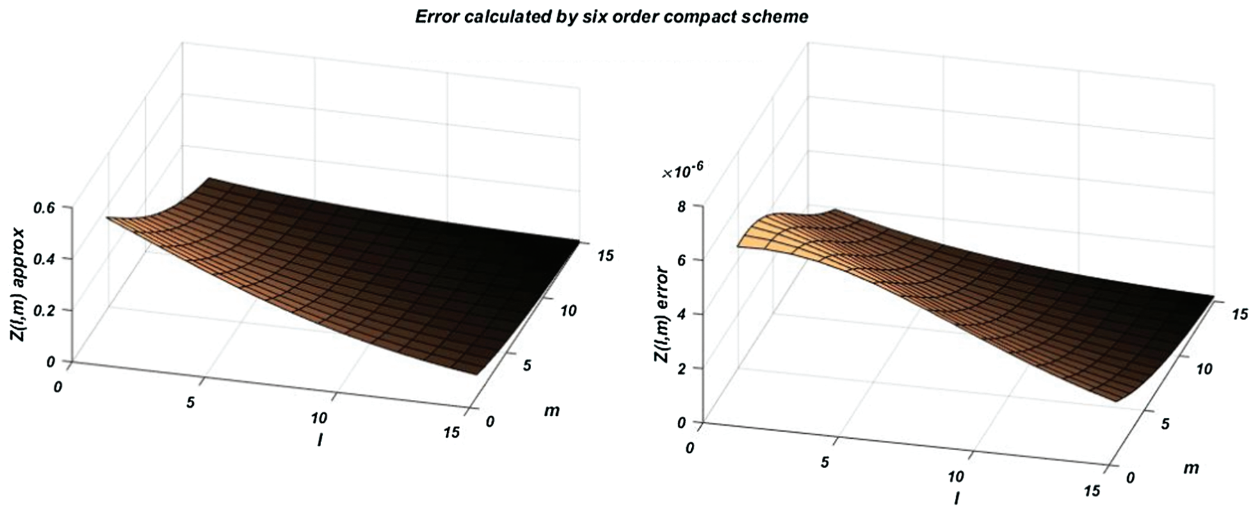

Figure 4: Results for error estimation by using 6th order scheme at $dt = 0.001$ & $\beta = 0.001$ at time 1

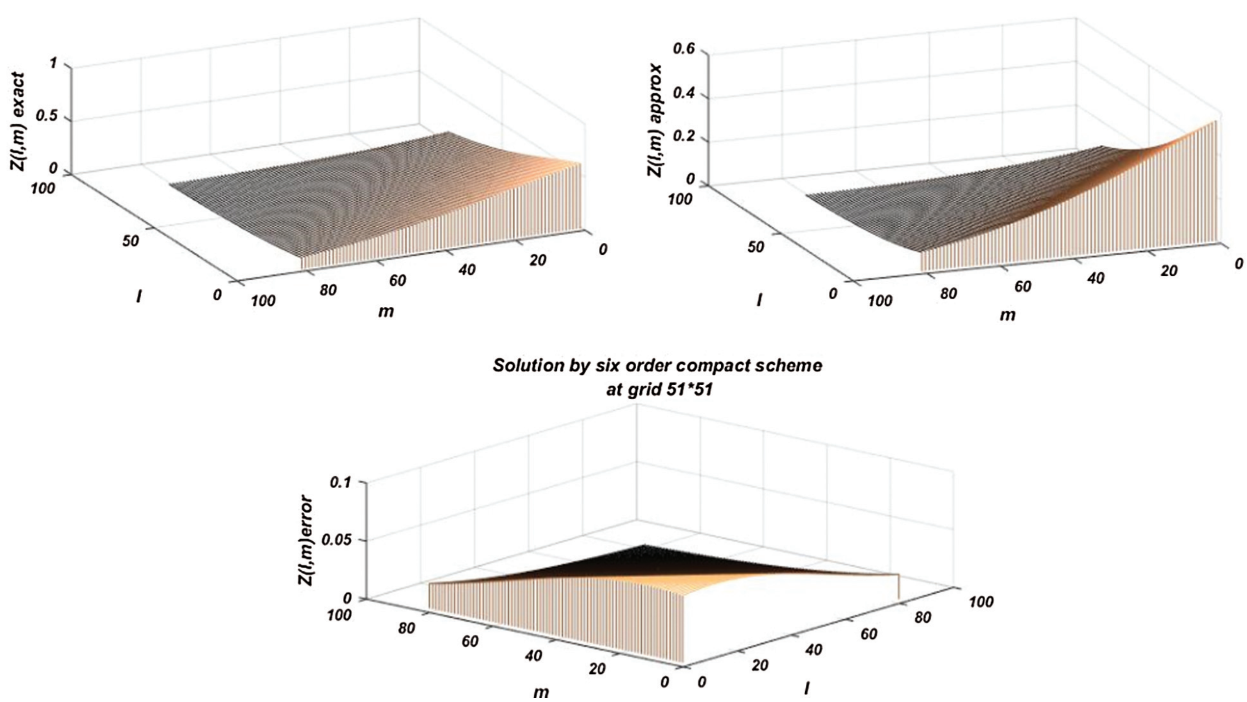

Figure 5: Results obtained by using 6th order scheme at $\beta = 0.0001$ at time level 0.5

6 Central Processing Unit Performance

A combinatorial logic circuit executes the mathematical operation for each function in the algorithm within the central processing unit. To establish the platform of CPU performance along physical memory transmission capacity is observed when the higher-order compact scheme is developed by using MATLAB software [35,39,42,43]. By increasing the grid size, the number of calculations is increased, and it is difficult to overcome such issue which can take a longer time to execute. Because of numerical schemes efficiency, the computational experiment is done on two different computer machines like Lenovo 6th generation having 2.4 GHz 8 cores and 16 GB memory along 5th generation Dell machine having 4 physical cores and 16 logical cores. Different feathers involved in two computational experiments can be analyzed from the following data tables.

Tab. 7 shows results for the different grid using 6th order compact scheme on Lenovo CPU oriented computational machine (MATLAB software).

Tab. 8 shows results for the different grid using 6th order compact scheme on DELL CPU oriented computational machine (MATLAB software).

Table 7: Central processing unit performance

Estimation of the time evolution using Lenovo idea pad 320 machine			
Grid size	Self-time (s)	Total time (s)	Calls C.Fn
17×17	80.307	170.579	120,102
31×31	101.345	250.345	487,882
51×51	150.23	380.34	1250,434

Table 8: Central Processing Unit Performance

Estimation of the time evolution using DELL machine			
Grid size	Self-time (s)	Total time (s)	Calls C.Fns
17×17	76.206	165.123	117,001
31×31	100.673	245.342	469,319
51×51	146.54	365.123	1211,729

To check the relative performance and execution time, here in this algorithm which used two machines, Dell and Lenovo, as follows:

$$Performance = \frac{1}{execution\,time} \tag{39}$$

where,

$$Relative_{perf} = \frac{perf_{machine1}}{perf_{machine2}} = \frac{Exe_{timemachine2}}{Exe_{timemachine1}} \tag{40}$$

The execution time of the Lenovo machine at (17×17) grid size is 170.579 s, and Dell machine execution time at the same grid size is 165.123 s. To calculate the relative performance we have

$$\frac{Exe_{lenove}}{Exe_{Dell}} = \frac{170.579\ s}{165.123} = 1.033\ s.$$

Results conclude that Dell machine is 1.033 faster than the Lenovo machine.

Clock cycle can be defined as:

$$CPU_{time} = no\ \ cycles \times clock\ \ cycle_{time} = \frac{no\ \ cycles}{clock_{rate}} \tag{41}$$

where $clock\ \ cycle_{time} = \dfrac{1}{clock_{rate}}$. For CPU time, the $clock_{rate} = 2\ \ GHz$, of Lenovo machines and clock rate, is 10 s, by increasing the $clock_{rate}$ means increase $clock_{cycle}$. The $clock_{rate}$ of Lenovo machine $= \frac{no\ \ clock_{cycle}}{no\ \ of\ \ CPU_{time}}$. To calculate the $clock_{rate}$ we have $clock_{cycle} = 1.2$. So

$$clock_{rate\,Dell} = \frac{1.2 \times clock_{cycleL}}{6\ \ s}$$

$$clock_{cycleL} = CPU_{timeL} \times clock_{rate_L} = 10 \times 2\ \ GHz = 20 \times 10^{09}_{\frac{cyc}{sec}}$$

Clock rate performance of Dell machine is, $CR_{Dell} = \dfrac{1.2 \times 20 \times^{09}}{6\ \ s} = 4\ \ GHz$

Comparison is performed to analyze Dell with Lenovo machines with both clock rate performance and relative performance. Thus MATLAB handles problems with care, and we can analyze results at each point of the loop and any iteration during computations.

7 Conclusion

Higher-order schemes for determining the two dimensional Burgers Huxley equation was developed in this paper. As it was not studied before by using such schemes of diffusive dissipation of errors. We came to know that the BH equation in two dimensional which is studied to find efficiency, accuracy and stability and by comparing with analytical and numerical approaches in terms of L_2, L_∞ & relative errors. It is evident from the fact that computed numerical experiments of two dimensional Burgers Huxley equation, solutions obtained by fourth and six order schemes are in good agreement with the analytical solutions. Figures and tables clearly show the tendency of fast and monotonic convergence of the results toward the analytical solution. Also, the computational discretization of the proposed model results in a sparse tridiagonal structure of the matrix, which can be overcome by the Thomas algorithm. Results lead to a remarkable improvement in accuracy, efficiency and computer performance which can be seen from data tables.

Acknowledgement: The authors are thankful to the anonymous referee for their suggestions and helpful comments that improved this article. We are also grateful to Vice-Chancellor, Air University, Islamabad, for providing an excellent research environment and facilities.

Funding Statement: The authors received no specific funding for this study.

Conflicts of Interest: The authors declare that they have no conflicts of interest to report regarding the present study.

References

[1] J. M. Burgers, "A mathematical model illustrating the theory of turbulence," *Advances in Applied Mechanics*, vol. 1, pp. 177–199, 1948.

[2] W. F. Ames, *Finite difference methods for partial differential equations*, vol. 22. New York: Academic Press, pp. 1–47, 1995.

[3] J. Noye, "Finite difference methods for partial differential equations," *North-Holland Mathematics Studies*, vol. 83, pp. 95–354, 1984.

[4] J. D. Logan, *An Introduction to Non-Linear Partial Differential Equations*. New York: Wily International Science, pp. 1–398, 2008.

[5] G. Sewell, *The Numerical Solution of Ordinary and Partial Differential Equations*. Canada: John Wiley and Sons, Inc., Hoboken, New Jersey, 2005.

[6] R. L. Burgen and J. D. Faries, "Numerical analysis," in: *Book*, 9th ed. Brooks/Cole, Cengage Learning, 2011.

[7] N. Taghizadeh, M. Akbari and A. Ghelichzadeh, "Exact solution of Burgers equations by homotopy perturbation method and reduced differential transformation method," *Australian Journal of Basic and Applied Sciences*, vol. 5, pp. 580–589, 2011.

[8] S. S. Ray and A. Gupta, "On the solution of Burgers–Huxley and Huxley equation using wavelet collocation method," *Computer Modelling in Engineering & Sciences*, vol. 91, pp. 409–424, 2013.

[9] J. E. Macas-Daz, "A modified exponential method that preserves structural properties of the solutions of the Burgers Huxley equation," *International Journal of Computer Mathematics*, vol. 95, no. 1, pp. 3–19, 2018.

[10] S. S. Ray and A. Gupta, "Comparative analysis of variational iteration method and Haar wavelet method for the numerical solutions of Burgers Huxley and Huxley equations," *Journal of Mathematical Chemistry*, vol. 52, pp. 1066–1080, 2014.

[11] R. Munafo, "Reaction diffusion by the Gray-Scott model: Pearsons parameterization," Unpublished Material, Available: http://mrob.com/pub/comp/xmorphia/index.html, under Creative Commons Attribution Non-Commercial 2.5 License, 2009.

[12] M. Saqib, S. Hasnain and D. Mashat, "Highly efficient computational methods for two dimensional coupled non-linear unsteady convection-diffusion problems," *IEEE Acess*, vol. 5, pp. 7139–7148, 2017.

[13] A. Gupta and S. S. Ray, "On the solutions of fractional Burgers Fisher and generalized Fisher equations using two reliable methods," *International Journal of Mathematics and Mathematical Sciences*, vol. 2014, pp. 1–16, 2014.

[14] A. Gupta and S. S. Ray, "Comparison between homotopy perturbation method and optimal homotopy asymptotic method for the soliton solutions of Boussinesq Burger equations," *Computer & Fluids*, vol. 103, no. 1, pp. 34–41, 2014.

[15] P. Vadasz and S. Olek, "Convergence and accuracy of Adomian decomposition method for the solution of Lorenz equation," *International Journal of Heat and Mass Transfer*, vol. 43, no. 10, pp. 1715–1734, 2000.

[16] H. N. A. Ismail, K. Raslan and A. A. Abd-Rabboh, "Adomian decomposition method for Burgers–Huxley and Burgers Fisher equations," *Applied Mathematics and Computation*, vol. 159, no. 1, pp. 291–301, 2004.

[17] I. Hashim, M. S. M. Noorani and M. R. S. Al-Hadidi, "Solving the generalized Burgers Huxley equation using the Adomian decomposition method," *Mathematical and Computer Modelling*, vol. 43, no. 1, pp. 1404– 1411, 2006.

[18] A. M. Wazwaz, "Analytic study on Burgers, Fisher, Huxley equations and combined forms of these equations," *Applied Mathematics and Computation*, vol. 195, no. 1, pp. 754–761, 2008.

[19] H. N. A. Ismail, K. Raslan and A. A. Abd-Rabboh, "Adomian decomposition method for Burgers Huxley and Burgers Fisher equations," *Applied Mathematics and Computation*, vol. 159, no. 1, pp. 291–301, 2004.

[20] I. Hashim, M. S. M. Noorani and M. R. S. Al-Hadidi, "Solving the generalized Burgers Huxley equation using the Adomian decomposition method," *Mathematical and Computer Modelling*, vol. 43, no. 11–12, pp. 1404–1411, 2006.

[21] I. Hashim, M. S. M. Noorani and B. Batiha, "A note on the Adomian decomposition method for the generalized Huxley equation," *Applied Mathematics and Computation*, vol. 181, no. 2, pp. 1439–1445, 2006.

[22] A. Molabahramia and F. Khani, "The homotopy analysis method to solve the Burgers Huxley equation," *Nonlinear Analysis: Real World Applications*, vol. 10, no. 2, pp. 589–600, 2009.

[23] O. Y. U. Efimova and N. A. Kudryashov, "Exact solutions of the Burgers Huxley equation," *Journal of Applied Mathematics and Mechanics*, vol. 68, no. 3, pp. 413–420, 2004.

[24] B. Batiha, M. S. M. Noorani and I. Hashim, "Application of variational iteration method to the generalized Burgers Huxley equation," *Chaos Solitons and Fractals*, vol. 36, no. 3, pp. 660–663, 2008.

[25] H. Gao and R. X. Zhao, "New exact solutions to the generalized Burgers–Huxley equation," *Applied Mathematics and Computation*, vol. 217, no. 4, pp. 1598–1603, 2010.

[26] R. K. Mohanty, W. Dai and D. Liu, "Operator compact method of accuracy two in time and four in space for the solution of time-dependent Burgers–Huxley equation," *Numerical Algorithms*, vol. 70, no. 3, pp. 591–605, 2015.

[27] M. Ablowitz, B. Fuchssteiner and M. Kruskal, "Topics in soliton theory and exactly solvable non-linear equations," in *Proc. of the Conf. on Non-linear Evolution Equations, Solitons and the Inverse Scattering Transform*, Oberwolfach, Germany, pp. 1–352, 1987.

[28] A. L. Hodgkin and A. F. Huxley, "A quantitative description of membrane current and its application to conduction and excitation in nerve," *Journal of Physiology*, vol. 117, no. 4, pp. 500–554, 1952.

[29] G. Adomian, "A review of the decomposition method in applied mathematics," *Journal of Mathematical Analysis and Applications*, vol. 135, no. 2, pp. 501–544, 1988.

[30] E. Y. Deeba and S. A. Khuri, "A decomposition method for solving the non-linear Klein–Gordon equation," *Journal of Computational Physics*, vol. 124, no. 2, pp. 442–448, 1996.

[31] X. Y. Wang, Z. S. Zhu and Y. K. Lu, "Solitary wave solutions of the generalized Burgers Huxley equation," *Journal of Physics A: Mathematical and General*, vol. 23, no. 3, pp. 271–274, 1990.

[32] A. M. Wazwaz, *Partial Differential Equations, Methods and Applications*. The Netherland: Balkema Publishers, 2002.

[33] M. Saqib, S. Hasnain and D. Mashat, "Computational solutions of three dimensional advection-diffusion equation using fourth-order time-efficient alternating direction implicit scheme," *AIP Advances*, vol. 7, pp. 85306, 2017.

[34] J. Jichun and Y. T. Chen, *Computational Partial Differential Equations Using Matlab*, 2^{nd} ed. Boca Raton, London, New York: Chapman and Hall/CRC Applied Mathematics and Nonlinear Science Series, 2020.

[35] Y. Huang, M. H. N. Skandari, F. Mohammadizadeh, H. A. Tehrani, S. G. Georgiev *et al.,* "Space-time spectral collocation method for solving Burgers equations with the convergence analysis," *Symmetry*, vol. 11, no. 12, pp. 1439, 2019.

[36] K. N. Tripathi, "Analytical solution of two-dimensional non-linear space time-fractional Burgers Huxley equation using fractional sub equation method," *National Academy Science Letters*, vol. 41, no. 5, pp. 295–299, 2018.

[37] J. Wei and M. Winter, "Asymmetric spotty patterns generated by Gray Scott Model in R2," *Studies in Applied Mathematics*, vol. 110, no. 1, pp. 63–102, 2003.

[38] K. Zhang, J. C. Wong and R. Zhang, "Second order implicit and explicit schemes to Gray Scott model," *Journal of Computational and Applied Mathematics*, vol. 213, no. 2, pp. 559–581, 2008.

[39] S. A. M. Tonekaboni, "Mathematical investigation of two-dimensional pattern formation," *International Journal of Biological Research*, vol. 2, no. 1, pp. 1–5, 2013.
[40] H. Guo, X. Zhuang and T. Rabczuk, "A deep collocation method for the bending analysis of Kirchhoff plate," *Computers, Materials & Continua*, vol. 59, no. 2, pp. 433–456, 2019.
[41] C. Anitescu, E. Atroshchenko, N. Alajlan and T. Rabczuk, "Artificial neural network methods for the solution of second-order boundary value problems," *Computers, Materials & Continua*, vol. 59, no. 1, pp. 345–359, 2019.
[42] E. Samaniego, C. Anitescu, S. Goswami, V. M. Nguyen-Thanh, H. Guo *et al.,* "An energy approach the solution of partial differential equations in computational mechanics via machine learning: Concepts, implementation and applications," *Computer Methods in Applied Mechanics and Engineering*, vol. 362, no. 15, pp. 112790, 2020.
[43] Pasha S. A., Nawaz Y., Arif M. S., "A third-order accurate in time method for boundary layer flow problems," *Applied Numerical Mathematics*, vol. 161, no. 1, pp. 13–26, 2021.